ChemElectroChem

Research Article
doi.org/10.1002/celc.202400449

Chemistry Europe
European Chemical Societies Publishing

www.chemelectrochem.org

Investigation on Psyllium Gum as a Bio-Based Binder for Silicon Anode in Lithium-Ion Batteries

Şebnem Cingisiz,[a] Emin Arca,[b] and Rezan Demir-Cakan*[a]

Silicon (Si) anode is of considerable interest in Li-ion batteries due to its high theoretical capacity (4200 mAh g^{-1}), abundant reserves in the earth, and environmentally friendly nature. Although Si anode has significant advantages, the electrode is prone to cracks due to large volume changes in its structure during discharge cycles in Li-ion batteries. Rapid capacity degradation occurs as a result of deterioration of the structural integrity of the electrode. Although binders are known to contribute to improving the electrochemical performance of anode materials, polyvinylidene fluoride (PVdF) used in commercial Li-ion batteries cannot maintain the mechanical stability of the Si anode during cycles due to weak Van der Waals interactions, which also dissolves in the flammable, explosive and volatile solvent N-Methyl-2-pyrrolidone (NMP). In this study, low cost, sustainable and environmentally green psyllium gum (PG) was extracted from psyllium husk and tested for the first time as a water-soluble binder for Si anode. According to galvanostatic charge/discharge tests, the Si-PG anode exhibits a capacity of 1415 mAh g^{-1} after 100 cycles at a voltage range of 0.01–1.5 V and current density of C/2, which is almost 3 times higher than the Si-PVdF anode (494 mAh g^{-1}).

Introduction

Li-ion batteries (LIBs) are widely used in portable electronic devices, electric vehicles (EVs), and renewable energy storage devices due to their extended cycle life, high power, and energy density.[1] The high demands for electric vehicles and emerging technologies, as well as the European Commission's awareness of the need to reduce gas emissions by approximately 55% by 2030 and achieve net zero emissions by 2050, require the improvement of Li-ion battery performance.[2]

Graphite is currently the most used anode material in commercial LIB applications, but its low theoretical capacity (372 mAh g^{-1}) is insufficient for the high demands and necessitates research into new high-performance anode materials.[3] Silicon, the second most abundant element on Earth, is one of the most promising high-performance anode materials because it is cost-effective, non-toxic and has low operation voltage (0.4 vs. Li/Li$^+$), and most importantly a very high theoretical capacity (4200 mAh g^{-1}).[4,5]

Although the theoretical capacity of silicon is high, in practical use the massive volume expansion (>300%) of silicon particles occurs during the lithiation process and this volume expansion of the Si anode during discharge causes many serious problems. For example, as a result of severe volume changes, the Si particles cannot withstand mechanical stress and pulverization occurs thus the contact between particles is reduced, resulting in delamination from the current collector surface.[6] Furthermore, the volume changes lead to continuous breakdown and formation of the SEI layer and an undesirable thick layer of SEI is formed on the electrode surface.[7] All these problems result in decreased coulombic efficiency, rapid capacity fading, and short cycle life.

The binders used in the electrodes play an important role in maintaining the mechanical integrity of the electrode, thereby contributing to electrical conductivity in Li-ion batteries.[8] As it is known, polyvinylidene difluoride (PVdF) binder provides effective results in graphite electrodes, but it is insufficient for high-capacity electrode materials such as Si, due to weak Van der Waals interactions in its structure. Furthermore, PVdF dissolves in a flammable, explosive, and toxic solvent N-Methyl-2-pyrrolidone (NMP) used in electrode preparation.[9] Nowadays, besides the effects of binders on electrochemical performance, their compatibility with sustainable green chemistry approaches is a very prominent factor in their use as binders. Therefore, functional, and water-soluble bio-based binders are preferred to overcome the disadvantages of Si anode. Brown algae-derived Na-alginate and cellulose ether-derived CMC contain abundant carboxylic and hydroxylic groups in their structures and their potential to form an effective bonding with Si particles makes them attractive for use as binders in Si anodes. These eco-friendly and bio-based binders have been reported to outperform conventional PVdF binders.[8,10] Recently, various environmentally friendly plant gums, have also been preferred as binders for Si anodes in LIBs. Guar gum (GG), a natural type of polysaccharide extracted from the seeds of the guar plant, is an example.[11] Xanthan gum (XG) is another remarkable natural polysaccharide that is cost-effective, has a double helical

[a] Ş. Cingisiz, R. Demir-Cakan
Department of Chemical Engineering, Gebze Technical University, 41400 Gebze, Kocaeli, Turkey
E-mail: demir-cakan@gtu.edu.tr

[b] E. Arca
Department of Chemical Engineering, Marmara University, Maltepe, İstanbul 34854, Turkey

Supporting information for this article is available on the WWW under https://doi.org/10.1002/celc.202400449

structure and is abundant in nature. Thanks to the trisaccharide side chains on the double helix structure of XG, it provides a strong adhesion with Si particles, similar to the adhesion mechanism of millipedes.[12] In 2021, Li et al. investigated the binding performance of peach gum obtained from the trunk and fruit of the peach tree on the Si anode electrode. In addition to this natural polysaccharide containing hydroxyl and carboxyl groups, the epichlorohydrin crosslinker was added to introduce a covalent bonding effect between the linkers.[13] Another interesting bio-based binder study was the okra gum obtained from okra pods. In 2021, Ling et al. tested the effect of okra gum (OG) on battery performance and reported that it performed better than the CMC binder.[14]

Psyllium, like the other bio-based polymers mentioned, is an environmentally friendly, low-priced, high-viscosity polysaccharide that contains abundant hydroxyl groups in its structure. It has a 70–85% water-soluble fiber content, is a laxative agent and dietary fiber supplement in addition to being employed in coating films, drug delivery systems, and as a stabilizer, thickener, and gel fillers in the food industry.[15–18] Herein, psyllium gum (PG) extracted from psyllium husk was used for the first time as a binder for Si anode. The contribution of this binder to the electrochemical performance of the Si electrode was evaluated using conventional PVdF as a benchmark, and comparable results with binders such as CMC, and CMC-SBR have been reported.

Results and Discussion

Psyllium gum extracted from the husk and seeds of the Plantago ovata plant is shown in Figure 1a. This natural polysaccharide consists mainly of 74.6% xylose and 22.6% arabinose and small amounts of glucose, galactose, mannose, uronic acid, and rhamnose (Figure 1b)[19.]

PG is a polysaccharide rich in hydroxyl and carboxyl groups, and these functional groups provide effective adhesion with the Si anode material. Therefore, bond interactions between Si nanopowders and PG binder were analyzed by FTIR spectroscopy (Figure 1c). The broad characteristic peak at 3328 cm^{-1} in PG is attributed to -OH stretching. There is a peak at 2928 cm^{-1} that corresponds to the -CH stretching vibrations of the CH_2 and CH_3 groups. Two peaks at 1640 cm^{-1} and 1379 cm^{-1} are asymmetrical COO^- stretching and symmetrical COO^- stretching vibrations of the hydrogen-bonded carboxylic groups, respectively. The sharp peak is located at 1033 cm^{-1} is ascribed to C–O or C–C stretching vibration.[20,21] The –OH stretching peak at ca. 3749 cm^{-1} in the FTIR spectrum of Si states the hydrogen bonds that enable the formation of Si-OH groups.[22] The peaks at 1106 cm^{-1} and 878 cm^{-1} are assigned to Si-O–Si asymmetrical and Si–O stretching vibration, respectively. These distinctive peaks in the Si FTIR spectrum demonstrate the outer SiO_2 layer on Si nanoparticles, which may develop as a result of exposure to oxygen in the atmosphere.[23] The -OH stretching peak in the FTIR spectrum of Si shifted to 3251 cm^{-1} at a relatively wider and lower wavelength in the spectrum of Si particles when used with PG binder. This change demonstrates

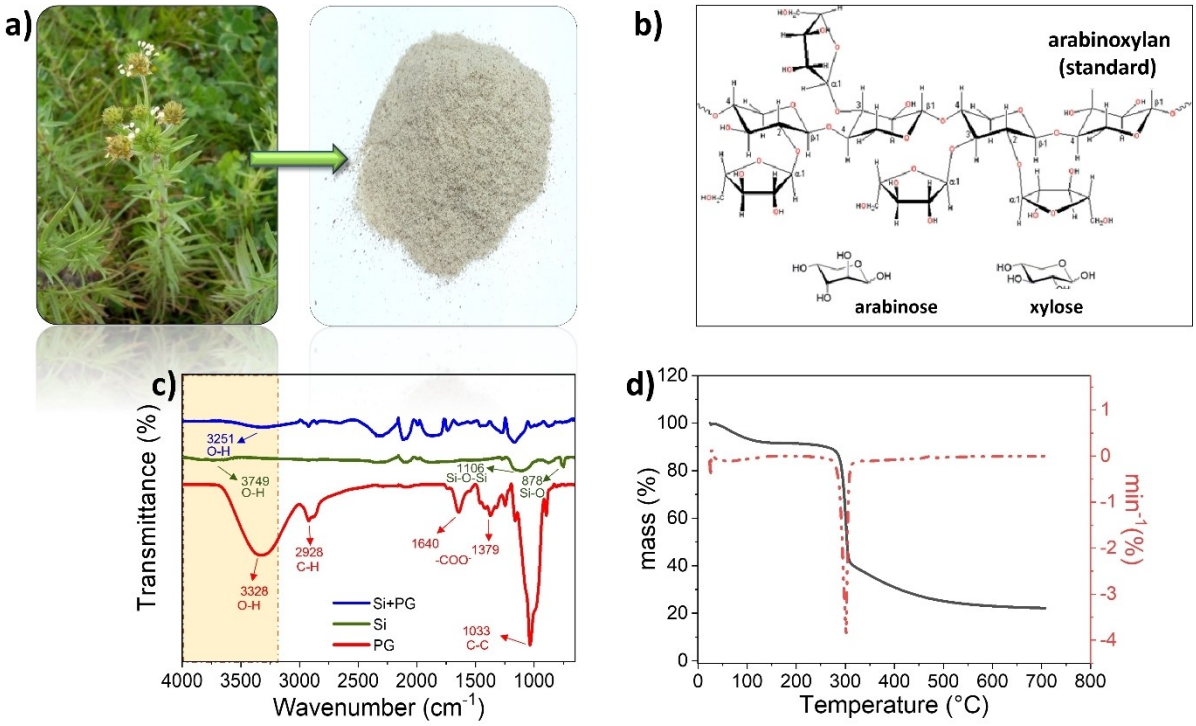

Figure 1. (a) The schematic illustration of psyllium husk, (b) the chemical structure of psyllium husk (c) FTIR Spectrum of psyllium gum (PG), Si nanoparticles, and PG mixed with Si nanoparticles, (d) thermogravimetric analysis (TGA) curve in black (left axis) and differential thermal analysis (DTA) curve in red (right axis) of PG under the inert nitrogen atmosphere.

that there is an increase in the hydrogen bond interactions between the functional groups in the PG binder's structure and the -OH groups on the surface of the Si particles.[11] These interactions in the electrode structure enhance mechanical integrity and may contribute to a more stable electrochemical performance.

The thermal stability of binders used in electrode materials is one of the important parameters affecting the electrochemical performance of batteries.[14] According to the TGA/DTA results in Figure 1d, the exothermic peak of PG at about 300 °C indicates the degradation of the psyllium backbone.[24,25] The relatively high decomposition temperature of PG makes it a potential binder for Li-ion battery applications under high operating temperature conditions.

Cyclic Voltammetry (CV) tests were performed in 1 M $LiPF_6$-EC-DMC FEC 5% electrolyte at a scan rate of 0.1 mV s^{-1} and a voltage range between 0.01 and 1.5 V to investigate the reaction mechanism of Si-PG and Si-PVdF electrodes with lithium ions. Figures 2a and b show that both electrodes exhibit almost similar CV profiles, in agreement with the literature.[13,26] The peak at 1.07 V seen in the first cathodic scan in the CV curves of Si-PG (less visible) and Si-PVdF anode material represents the formation of the SEI layer caused by electrolyte degradation.[27] These peaks disappeared after the second scan, which may explain the absence of side reactions in the operating voltage range and electrochemical stability with the stable SEI.[28] The sharp peak at ~0.01 V in the first cathodic scan of the Si-PG electrode given in Figure 2a is attributed to the formation of Li_xSi alloy phases.[29] In subsequent cycles, silicon undergoes a structural transformation and a new peak appears at 0.17 V in the cathodic scan.[30] These peaks, resulting from the amorphization of silicon and the formation of crystalline LiSi

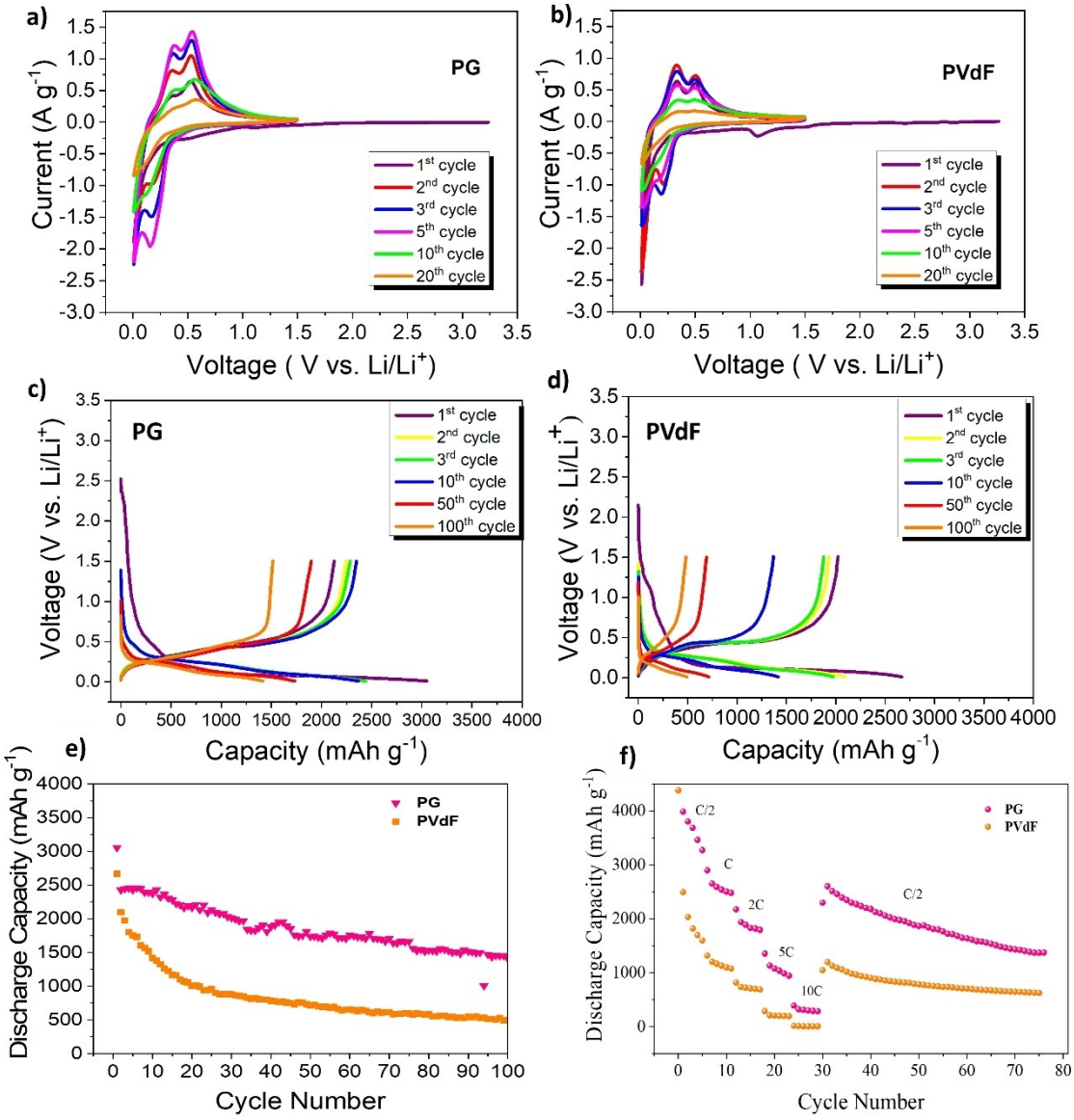

Figure 2. Cyclic voltammetry (CV) curves of (a) Si-PG electrode and (b) Si-PVdF electrode at a scanning rate of 0.1 mV s^{-1} and a voltage range of 0.01–1.5 V. Discharge/charge curves of (c) Si-PG electrode and (d) Si-PVdF electrode. (e) Discharge capacity-cycle number curves for PG and PVdF binders, at a current density of C/2. (f) The rate performance of Si-PG and Si-PVdF electrodes.

alloys, represent the gradual formation of $Li_{12}Si_7$ and $Li_{15}Si_4$ phases.[31] The anodic scan's peaks at 0.36 V and 0.53 V, respectively, describe how the Li_xSi phase changes into amorphous Si, a process known as delithiation. When the first three scans are examined, it is observed that the redox currents of the Si-PG anode gradually increase while those of the Si-PVdF anode starts to decrease after the second cycle. The gradual increase in current values indicates that more Si is used during the activation. To compare the redox performances of Si-PG and Si-PVdF electrodes, current values are given per gram of Si are given in CV curves where the Si-PG anode shows a larger current value than the Si-PVdF electrode within the same voltage ranges, indicating a better energy capacity with higher electrochemical activity.[32,33]

The galvanostatic charge/discharge cycles of the Si-PG and Si-PVdF electrodes between the voltages of 0.01 V to 1.5 V at the rate of C/2 are given in Figure 2c and d, respectively. Si-PG electrode provided the first discharge capacity of 3050 mAh g^{-1} with an initial irreversible capacity loss of 20.5 %, and through the later Si-PG anode exhibited a good cycling performance with a capacity retention of 46.4 % at the end of 100 cycles. On the other hand, when the discharge/charge profile of the Si electrode prepared with conventional PVdF binder is tested under the same conditions, it is seen that a capacity of 2670 mAh g^{-1} and an irreversible capacity of 21.5 % is achieved in the first cycle. Moreover, the discharge capacity decreased to 494 mAh g^{-1} after 100 cycles, retaining only 18.50 % of its capacity (Figure 2d). Although PVdF is preferred in commercial Li-ion batteries due to its electrochemical stability and good adhesion to conventional electrode materials, it has been reported that when used with electrode materials with high energy density such as Si anode, it cannot withstand large volume changes during lithiation/delithiation and fails to maintain mechanical integrity due to weak Van der Waals interactions.[34] This results in poor electronic conductivity between the Si particles and the conductive carbon/current collector and explains the rapid capacity decay.[35] Thus, the Si-PG anode material resulted a higher capacity value and better capacity retention performance after 100 cycles (Figure 2e). Si-PG and Si-PVdF anodes were also tested at varying current densities from C/2 to 10 C (Figure 2f). The discharge capacity of the Si-PG anode is much higher than that of Si-PVdF at all applied currents and a capacity difference of 742 mAh g^{-1} was observed between Si-PG and Si-PVdF anodes after 75 cycles at C/2 rate. To the best of our knowledge, the electrochemical performance of Si anode material with PG binder has not been previously discussed in the literature. PG is rich in carboxyl and hydroxyl groups, which provide a strong bonding effect on the Si electrode and maintain structural integrity, which is critical for electrochemical stability. The electrochemical performance of the PG binder was also compared with CMC and CMC-SBR, and compatible results were obtained, thus concluding that PG can be proposed as an alternative binder (Figure S1).

It is known that the binders used in the preparation of the electrode material affect the transfer rate of Li^+ inside the cell and the internal resistance of the electrode material.[36] For this reason, to further examine the effects of PG and PVdF binders on the electrochemical performance of the Si anode in Li-ion batteries, the impedance behavior of Si-PG and Si-PVdF anodes was investigated. Nyquist plots show the results of the EIS experiment before and after C-rate tests (75 cycles) of Si-PG and Si-PVdF electrodes (Figures 3a and b). Depressed semi-circles

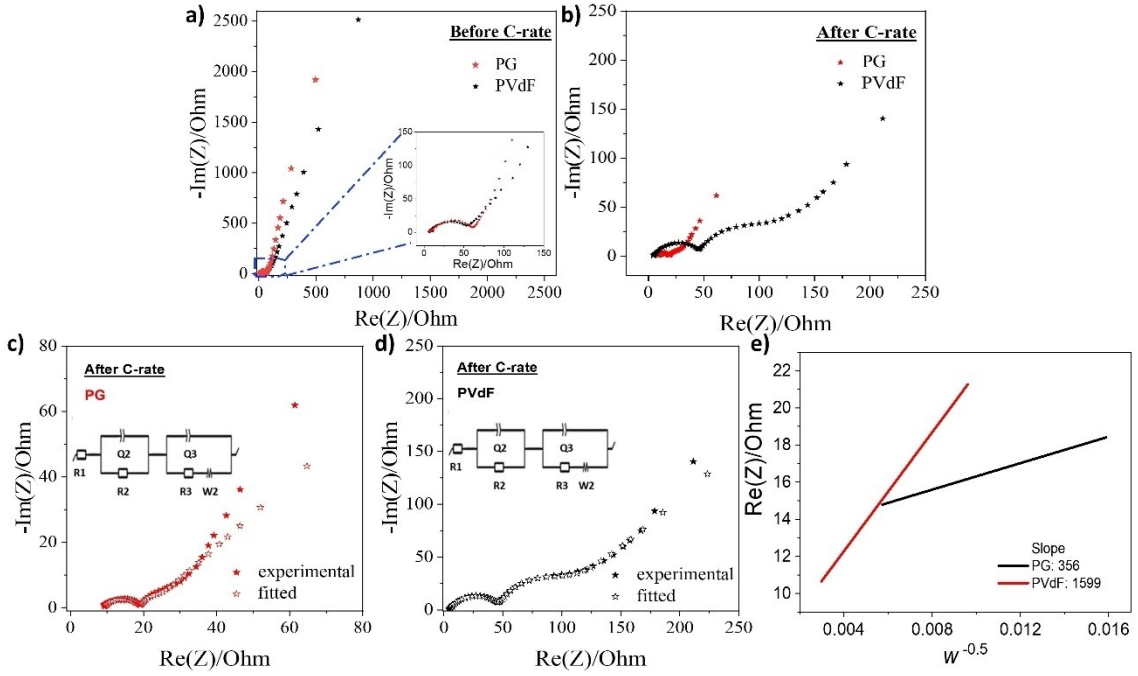

Figure 3. Electrochemical impedance spectrum (EIS) of Si-PG and Si-PVdF electrodes (a) before and (b) after C-rate tests (After 75 cycles). The experimental and equivalent circuit fitting curves of the (c) Si-PG and (d) Si-PVdF after C-rate. (e) The linear relationship between Re(Z) and $\omega^{-0.5}$ at low-frequency region for the Si-PG and S-PVdF.

starting from the high-frequency region in the Nyquist plots are attributed to the solid electrolyte interface resistance (R_{SEI}) occurring at the electrode and electrolyte interface in this region, and the mid-frequency region towards the end of the circle is attributed to the charge transfer resistance (R_{CT}).[37,38]

As seen in the impedance results, the depresses semi-circle diameters before cycle are very close to each other. After C-rate tests, EIS data were fitted for both electrodes. According to the fitted EIS data given in Figure 3c and d, R_{total} for Si-PG electrode was obtained 21.46 Ω (R_1: 9.063 Ω, R_2: 2.365 Ω and R_3: 10.03 Ω) is lower than that of Si-PVdF electrode R_{total}: 102.11 Ω (R_1 : 4.33 Ω, R_2 45.47 Ω and R_3 52.31 Ω). In Nyquist plots, the line in the low-frequency region following the semicircle indicates the Warburg impedance at which the Li^+ diffusion can be calculated.[39] The equation in which the diffusion coefficient (D_{Li+}) is inversely proportional to the Warburg coefficient (σ) is as follows.

$$D_{Li^+} = \frac{R^2T^2}{2n^4A^2F^4C^2\sigma^2} \quad (1)$$

where R is the gas constant (8.314 J mol^{-1} K^{-1}), T is the temperature (298 K), n is the number of electrons transferred in the electrochemical reaction (n = 1), A is the surface area of the electrode material (1.21 cm^2), F is Faraday constant 96500 C mol^{-1}) and C is the molar concentration of Li^+ in the electrode. The slope of the line equation obtained from the graph of $\omega^{-0.5}$ against Re(Z) in Figure 3**e** gives the Warburg factor. D_{Li+} values for Si-PG and Si-PVdF anodes were calculated as 7.94×10^{-12} cm^2 s^{-1} and 3.52×10^{-12} cm^2 s^{-1}, respectively. As a result of the comparison of the impedance behavior of the two anode materials, it was concluded that the PG binder provides a stable SEI layer, fast electron transfer, and fast Li^+ diffusion, leading to better electrochemical performance and stability.

SEM was used to further investigate the morphological properties of Si-PG and Si-PVdF anode materials. Figure 4a and b show the SEM images of Si-PVdF and Si-PG anode materials before electrochemical treatment, and Figure 4c and d show after 100 charge/discharge cycles at C/2 rate, respectively. After 100 cycles, cracks appeared on both electrode surfaces due to the volume changes in the Si anode during cycling, but the large cracks on the Si-PVdF electrode are more noticeable. The PG binder performed better in maintaining the mechanical integrity of the electrode during cycling, and this result supports that the PG binder has a significant advantage for the Si anode electrode in Li-ion batteries over PVdF.

Furthermore, the stability of the electrodes at nanometer dimensions is presented with Transmission Electron Microscopy (TEM) images. Figure 5a shows the structure of silicon nanoparticles demonstrating ca. 150–200 nm size spherical Si nanoparticles. Figure 5b and d show the TEM images of Si-PG and Si-PVdF electrodes before cycling, respectively. After 50 cycles, the structural integrity of the Si-PG electrode appears to be better stabilized (Figure 5c), while the Si-PVdF electrode shows relative structural degradation (Figure 5e). This suggests that PG can bind silicon nanoparticles and conductive carbon together quite well, allowing for better adhesion on the surface of the current collector.

Figure 6a shows comparison images of Si-PG and Si-PVdF electrodes before electrochemical treatment and after 100 cycles. The Si-PVdF electrode is well coated on the copper surface, however in some regions of the electrode surface the coating peels off the copper foil, while the coating of the Si-PG electrode appears homogeneous and smooth. Comparing the optical images of both anode materials after 100 cycles at C/2 current density, it can be seen that the Si-PVdF electrode surface is more deformed and the coating flakes off. This can be associated with the adhesion properties of the binders used in the preparation of the anode materials, more precisely, the PG

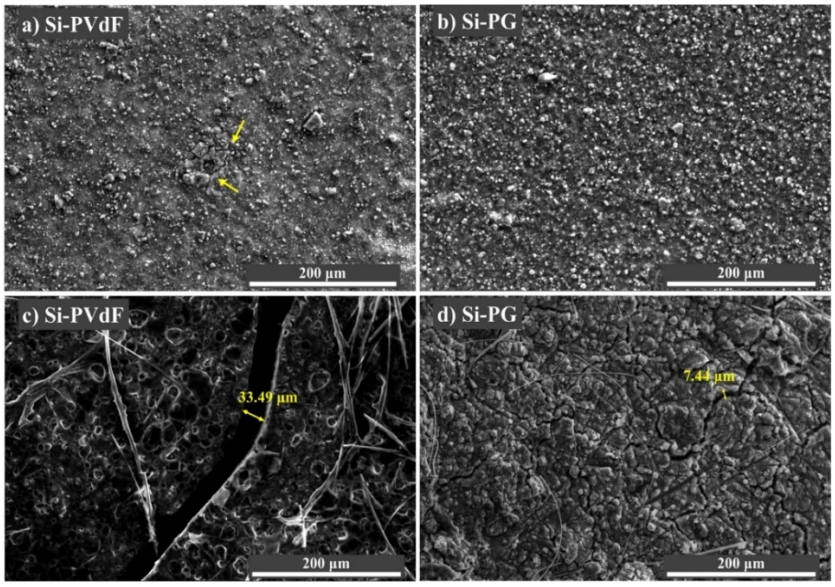

Figure 4. SEM images of Si-PVdF and Si-PG electrodes (a, b) before cycle and (c, d) after 100 cycles, respectively.

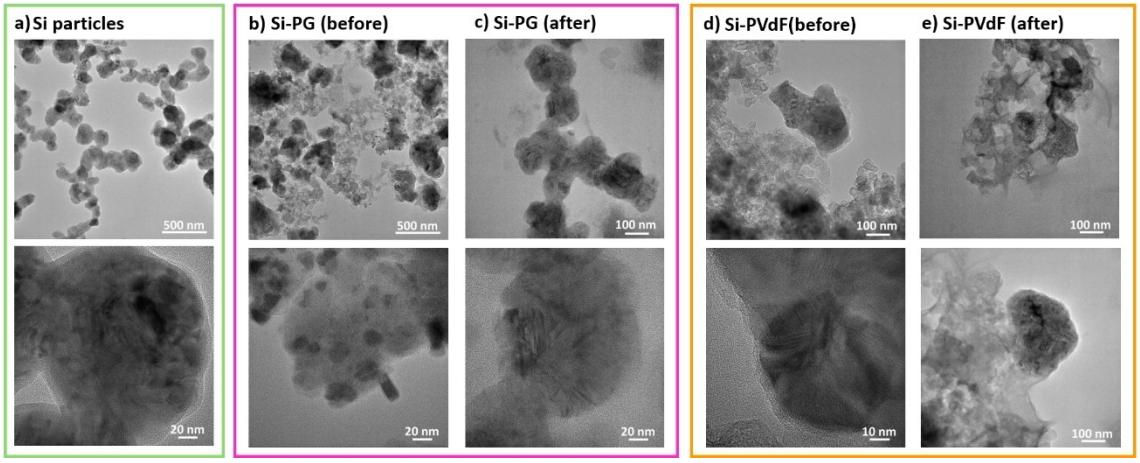

Figure 5. TEM images of silicon nanoparticles (a), Si-PG electrodes before and after 50 cycles (b, c), Si-PVdF electrodes before and after 50 cycles (d, e).

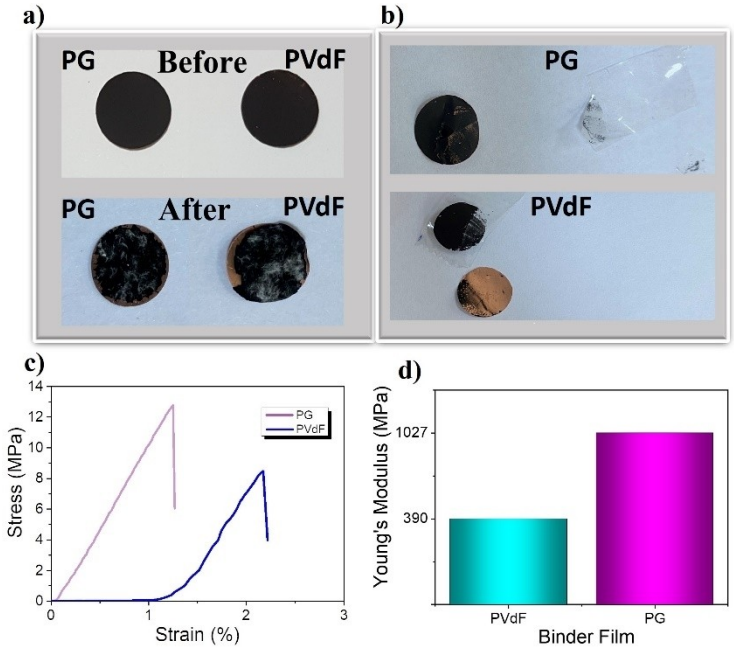

Figure 6. Optical images of Si-PG and Si-PVdF (a) before the cycle and after 100 cycles (b) electrodes after peel-test. (c) Stress-strain curve and, (d) Young's Modulus of PVdF and PG binder respectively.

binder provided stronger adhesion of the active material and conductive carbon to the copper foil compared to PVdF.

The binding performance of the binders used in the electrode materials can also be examined by the peel test before the electrochemical cycle. The physical stability of the electrode was tested by sticking a piece of tape on the surface of the two anode materials and pulling with the same force as much as possible. Optical images of the peeling-test result of the Si-PG and Si-PVdF electrodes are given in Figure 6b. The Si-PG electrode coating adhered well to the copper surface and could not be peeled off with the tape, while almost all of the Si-PVdF electrode adhered to the tape surface. This supports the conclusion that the adhesion strength of the PG binder is higher than that of PVdF.

As previously mentioned, binders play a critical role in maintaining mechanical stability during the cycles. Tensile test was performed to characterize the mechanical strength of PG and PVdF binders. As demonstrated in Figure 6c, the stress values of PG and PVdF films are 12.76 MPa and 8.48 MPa, while the strain (%) values are 1.25% and 2.17%, respectively. Compared with PG and PVdF binder, PG exhibits less stretching and has higher stress strength. The ratio of the stress and strain values obtained from the tensile test of the binder films determines Young's Modulus.[40] The Young's Modulus of PVdF and PG are 1027 MPa and 390 MPa, respectively (Figure 6d). Low Young's Modulus binders cannot maintain the strength of the electrode due to poor stress distribution. This results in rapid capacity decay throughout the electrochemical cycle. In this context, it has been reported in the literature that binders

with superior electrochemical performance have higher Young's Modulus values.[41,42]

Conclusions

This study aims to contribute to the literature by proposing a cost-efficient, electrochemically stable binder that supports the green chemistry concept. In this context, we used psyllium gum (PG), the husk of psyllium seeds, as a binder in the silicon anode for the first time. According to the galvanostatic charge/discharge tests performed at the C/2 rate, the PG binder, with a discharge capacity of 1415 mAh g^{-1} and capacity retention of 46.4% after 100 cycles. The hydroxylic and carboxylic functional groups in its structure cause it to exhibit good binding properties. The binder with the lowest electrochemical performance among the binders studied is PVdF with a capacity of 494 mAh g^{-1} and a capacity retention of 18.50%. As a general result, it was claimed that PG binder, which is environmentally friendly, low-cost, and has good electrochemical performance, can be used as an alternative binder to PVdF binder in Si anode material for Li-ion batteries.

Experimental Section

Materials

Silicon (Si) nanopowder (Nanografi) as an active material, Ketjen Black (KB) (EC-300 J, AkzoNobel) and Super P (SP) (Timcal) as conductive carbon additives, carboxymethyl cellulose CMC (Doga Nanobiotech), carboxymethyl cellulose-styrene butadiene rubber (CMC-SBR), psyllium husk powder (Vegrano), and polyvinylidene difluoride PVdF (Alfa Aesar) as binders were used for the preparation of anode electrode. N-Methyl-2-pyrrolidone NMP (Alfa Aesar) was used as a solvent for PVdF binder and for the other binders distilled water was used, respectively. Ethylene carbonate EC (Sigma Aldrich), dimethyl carbonate DMC (Sigma Aldrich), fluoroethylene carbonate FEC (Alfa Aesar), and lithium hexafluorophosphate ($LiPF_6$) (Sigma Aldrich) were used for the electrolyte preparation.

PG Binder Preparation

Psyllium husk powder and distilled water were mixed with a weight ratio of 0.05:10 at 300 rpm for 1 h at 70 °C and the gelled mixture was stirred overnight at room temperature. After that, the mixture was centrifuged at 5500 rpm for 20 minutes to remove the particulate materials from the gummy structure. After centrifugation, a clear PG phase free of any impurities was obtained, transferred to a Teflon dish, and oven to dry. The dry sample was powdered and kept for future use.

Electrode Preparation

All negative electrode materials were prepared by mixing Si active material, KB conductive carbon additive, SP conductive carbon additive, and binder in a weight ratio of 60:20:20, respectively. First, Si and KB were mixed (weight ratio 3:1) in Ball Mill (BM) (Retsch MM400) for 30 min at a frequency of 25 Hz. Then, SP and binder were added to this mixture and grounded in a mortar for 10 minutes. The slurry obtained was mixed for 24 h at 300 rpm and in ambient condition. Afterward, the homogeneous slurry was coated on copper foil with the help of a doctor-blade, and electrode preparation was carried out. The electrode was dried in a vacuum oven at 80 °C for overnight. The amount of active material loading on the copper foil (10 μm thick) in the disc electrodes (11 mm) was around 0.5–0.8 mg cm^{-2} (~22–24 μm thickness, excluding Cu current collector). The same processes were repeated using different binders (PG, PVdF, CMC, and CMC-SBR).

Material Characterization

Fourier Transform Infrared Spectroscopy (FTIR) (Perkin Elmer Spectrum 100) was used for the analysis of the bond structure of PG binder, Si particles, and PG–Si mixture (Si and PG were mixed in water and the dried powder was characterized). The thermal behavior of the PG binder was investigated by Thermogravimetric Analysis (TGA)/Differential Thermal Analysis (Mettler Toledo) up to 700 °C under Ar atmosphere. The peel-test was performed to examine the binding performance and mechanical stability of PG and PVdF binders. Scanning Electron Microscopy (SEM) (Thermo Fisher Quattro ESEM FE-SEM) was used to examine the morphological properties of Si-PVdF and Si-PG anode materials. TEM (JEOL JEM 2100 F) was used to observe the structure of Si-PVdF and Si-PG electrodes. Tensile test machine (Devotrans DVT BP D NN) was used to characterize the mechanical strength of PVdF and PG binders. The tensile process was performed in the vertical position at a speed of 5 mm min^{-1}.

Electrochemical Measurements

The CR2025 coin cell and Swagelok-type cell were assembled in a glove box under high-purity Ar. The electrolyte solution was prepared by mixing 1 M $LiPF_6$ salt in EC and DMC (volume ratio of 1:1) solvents and 5% FEC additive at 300 rpm for 1 day. Metallic lithium was used as both reference and counter electrodes. In a galvanostatic charge/discharge cycle, Li-ion cells were tested in a voltage range of 0.01–1.5 (vs. Li/Li^+) and a rate of C/2 in Neware battery test station. Different current rates (C/2, 1 C, 2 C, 5 C, 10 C, and C/2, 1 C = 4.2 A/g) were applied for C-rate performance tests. Cyclic voltammetry (CV) measurements were performed at a scanning rate of 0.1 mV s^{-1}. Electrochemical Impedance Spectroscopy (EIS) experiments were carried out at the VMP3 Bio-Logic test station in the frequency range of 10 mHz to 1 MHz and at an AC amplitude of 5 mV, at the open-circuit voltage of the cells and after C-rate cycles.

Acknowledgements

SC expresses her gratitude to TÜBİTAK 2211-A National Doctoral Fellowship Programme for their financial support.

Conflict of Interests

The authors declare no conflict of interest.

Data Availability Statement

The data that support the findings of this study are available from the corresponding author upon reasonable request.

Keywords: Li-ion battery · Silicon anode · Psyllium gum binder · Electrochemical performance

[1] B. Diouf, R. Pode, *Renewable Energy* **2015**, *76*, 375–380.
[2] J. Amici, et al., *Adv. Energy Mater.* **2022**, *12* (17), 2102785.
[3] P. Nzereogu, A. Omah, F. Ezema, E. Iwuoha, A. Nwanya, *Appl. Surf. Sci. Adv.* **2022**, *9*, 100233.
[4] M. A. Rahman, G. Song, A. I. Bhatt, Y. C. Wong, C. Wen, *Adv. Funct. Mater.* **2016**, *26* (5), 647–678.
[5] R. Xu, et al., *Nano Energy* **2017**, *39*, 253–261.
[6] S. Choi, T.-W. Kwon, A. Coskun, J. W. Choi, *Science* **2017**, *357* (6348), 279–283.
[7] T.-W. Kwon, J. W. Choi, A. Coskun, *Chem. Soc. Rev.* **2018**, *47* (6), 2145–2164.
[8] C. Wang, H. Wu, Z. Chen, M. T. McDowell, Y. Cui, Z. Bao, *Nat. Chem.* **2013**, *5* (12), 1042–1048.
[9] J. T. Li, et al., *Adv. Energy Mater.* **2017**, *7* (24), 1701185.
[10] I. Kovalenko, et al., *Science* **2011**, *334* (6052), 75–79.
[11] J. Liu, Q. Zhang, T. Zhang, J. T. Li, L. Huang, S. G. Sun, *Adv. Funct. Mater.* **2015**, *25* (23), 3599–3605.
[12] Y. K. Jeong, T.-W. Kwon, I. Lee, T.-S. Kim, A. Coskun, J. W. Choi, *Energy Environ. Sci.* **2015**, *8* (4), 1224–1230.
[13] Z. Li, et al., *Nano Energy* **2021**, *79*, 105430.
[14] H. Y. Ling, et al., *Sustainable Mater.Technol.* **2021**, *28*, e00283.
[15] S. Cui, Y. Wu, H. Ding, *Fibre-Rich and Wholegrain Foods: Improving Quality, Woodhead Publishing Series in Food Science, Technology and Nutrition: Number 237*, **2013**, Chapter 5, 96–119.
[16] Q. Guo, S. W. Cui, Q. Wang, J. C. Young, *Carbohydr. Polym.* **2008**, *73* (1), 35–43.
[17] M. K. Patel, B. Tanna, H. Gupta, A. Mishra, B. Jha, *Int. J. Biol. Macromol.* **2019**, *133*, 190–201.
[18] S. Kulkarni Vishakha, D. Butte Kishor, S. Rathod Sudha, *Int. J. Res. Pharm. Biomed. Sci* **2012**, *3* (4), 1597–1613.
[19] D. Kumar, J. Pandey, P. Kumar, V. Raj, *Curr. Synthetic Sys. Biol.* **2017**, *5* (134), 2332–0737.1000134.
[20] A. Farahnaky, H. Askari, M. Majzoobi, G. Mesbahi, *J. Food Eng.* **2010**, *100* (2), 294–301.
[21] B. Singh, N. Chauhan, S. Kumar, *Carbohydr. Polym.* **2008**, *73* (3), 446–455.
[22] H. Chen, et al., *Nano Energy* **2021**, *81*, 105654.
[23] Z. Liu, et al., *RSC Adv.* **2016**, *6* (72), 68371–68378.
[24] M. K. Patel, B. Tanna, A. Mishra, B. Jha, *Int. J. Biol. Macromol.* **2018**, *118*, 976–987.
[25] A. Kumari, B. Kaith, A. Singha, S. Kalia, *Adv. Mater. Lett.* **2010**, *1*, 123–128.
[26] J. Xu, Q. Zhang, Y.-T. Cheng, *J. Electrochem. Soc.* **2015**, *163* (3), A401.
[27] L. Yu, et al., *J. Phys. Chem. Solids.* **2019**, *135*, 109113.
[28] J. Nam, E. Kim, *Sci. Rep.* **2020**, *10* (1), 14966.
[29] L. Yan, et al., *ACS Appl. Mater. Interfaces* **2017**, *9* (44), 38159–38164.
[30] K. Zhang, Y. Xia, Z. Yang, R. Fu, C. Shen, Z. Liu, *RSC Adv.* **2017**, *7* (39), 24305–24311.
[31] W. Sun, L. Wan, X. Li, X. Zhao, X. Yan, *J. Mater. Chem. A* **2016**, *4* (28), 10948–10955.
[32] S. Bolloju, Y.-L. Chang, S. U. Sharma, M.-F. Hsu, J.-T. Lee, *Electrochim. Acta* **2022**, *419*, 140390.
[33] A. Uctepe, et al., *Solid State Ionics* **2020**, *354*, 115409.
[34] C. C. Nguyen, T. Yoon, D. M. Seo, P. Guduru, B. L. Lucht, *ACS Appl. Mater. Interfaces* **2016**, *8* (19), 12211–12220.
[35] Y. Wang, D. Dang, D. Li, J. Hu, X. Zhan, Y.-T. Cheng, *J. Power Sources* **2019**, *438*, 226938.
[36] H. Wang, et al., *ACS Sustainable Chem. Eng.* **2020**, *8*(34), 12799–12808.
[37] J. Fei, Q. Sun, Y. Cui, J. Li, J. Huang, *J. Electroanal. Chem.* **2017**, *804*, 158–164.
[38] Y. Gao, et al., *ACS Sustainable Chem. Eng.* **2019**, *7* (19), 16274–16283.
[39] K. Rajeev, J. Nam, W. Jang, Y. Kim, T.-H. Kim, *Electrochim. Acta* **2021**, *84*, 138364.
[40] J. D. Lord, R. Morrell, *Metrologia* **2010**, *47* (2), S41.
[41] A. Casimir, H. Zhang, O. Ogoke, J. C. Amine, J. Lu, G. Wu, *Nano Energy* **2016**, *27*, 359–376.
[42] X. Jiao, et al., *Adv. Funct. Mater.* **2021**, *31* (3), 2005699.

Manuscript received: July 9, 2024
Revised manuscript received: July 26, 2024
Version of record online: ■■, ■■

RESEARCH ARTICLE

Psyllium Gum (PG), derived from psyllium husk, is an environmentally friendly, abundant, inexpensive, water-based binder containing carboxylic and hydroxyl groups. PG has the potential to form strong bonds with Si particles and thus helps to maintain material integrity after severe volume changes. Due to these properties, it can be considered an alternative binder for alloy anode materials in alkali-ion batteries.

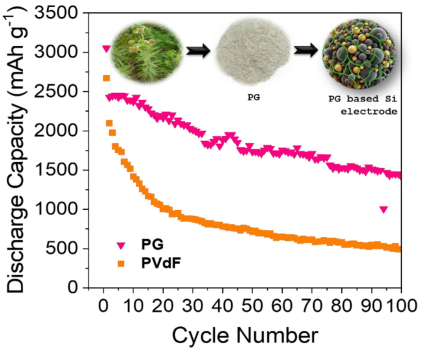

*Ş. Cingisiz, E. Arca, R. Demir-Cakan**